



Do sulfate and nitrate coatings on mineral dust have important effects on radiative properties and climate modeling?

S. E. Bauer,^{1,2} M. I. Mishchenko,² A. A. Lacis,² S. Zhang,^{2,3} J. Perlwitz,^{2,4} and S. M. Metzger⁵

Received 12 December 2005; revised 20 October 2006; accepted 14 November 2006; published 24 March 2007.

[1] Coating of mineral dust particles by air pollutants leads to core-mantle particles. These composite aerosols could interact differently with atmospheric radiation than the uncoated dust. In our simplified radiative calculations we assumed that a spherical dust core is covered uniformly by a liquid refractive material, such as sulfate or nitrate. Theoretical calculations of optical properties of such particles show that the single-scattering albedo and the asymmetry parameter of core-mantle aerosols only differ significantly from uncoated dust if coating layers exceed 20% of the radius of the dust core. Global simulations of sulfate/nitrate-coated dust particles show that the thickness of the shell can be expected to range from 0 to 20% of the radius of the dust core. The result of this work is that mineral dust particles can be treated as external mixture within radiative calculations but the coating processes lead to changed loads in sulfate, nitrate, and mineral dust aerosol loads and therefore change their impact on Earth radiation. The combined anthropogenic forcing of dust, nitrate, and sulfate aerosols is -0.1 W/m^2 ; however, excluding heterogeneous interactions leads to a 3 times larger negative forcing.

Citation: Bauer, S. E., M. I. Mishchenko, A. A. Lacis, S. Zhang, J. Perlwitz, and S. M. Metzger (2007), Do sulfate and nitrate coatings on mineral dust have important effects on radiative properties and climate modeling?, *J. Geophys. Res.*, 112, D06307, doi:10.1029/2005JD006977.

1. Introduction

[2] The terrestrial atmosphere often contains mixtures of different aerosol particle types, including internal, semi-external, and external mixtures, as defined by *Mishchenko et al.* [2004b]. The identification of the state of mixing is important because the latter may affect particle radiative properties. In an external or semiexternal mixture, each aerosol particle consists of a single material, and so can be considered homogeneous. Internal mixtures contain more than one material and sometimes coexist in different phases. The formation of an internally mixed particle can be caused by coagulation, coalescence of particles in clouds, and gas-aerosol transfer reactions on aerosol surfaces. The global characterization of the mixing state of aerosols is extremely difficult, because essentially all existing observations are bulk measurements providing no information on the aerosol chemical composition [*Mishchenko et al.*, 2004a].

[3] In situ analyses of individual particles can provide detailed information such as size, shape, and composition, but are very time consuming, difficult to perform, and limited to a specific location. As a result, information about the mixing state of atmospheric aerosols is very scarce, although the existing observations show clearly that a significant fraction of the atmospheric aerosols may exist as particle mixtures [*Buseck and Posfai*, 1999; *Buseck et al.*, 2000; *Li et al.*, 2003a, 2003b; *Trochkin et al.*, 2003].

[4] Most atmospheric radiation models still assume aerosols as externally mixed. However, many research groups are developing more complex simulation approaches which should be able to predict more accurately the chemical composition and mixing state of aerosol particles [*Gong et al.*, 2003; *Stier et al.*, 2005; *Jacobson*, 2001]. Hence it is timely and important to analyze theoretically the radiative properties of various types of aerosol mixtures.

[5] *Mishchenko et al.* [2004b] compared the scattering and radiative properties of semiexternal and external mixtures. By definition, aerosols are mixed semiexternally when they are in physical contact but not embedded in each other. This kind of particles mainly form through coagulation. *Mishchenko et al.* [2004b] found that the optical properties of a semiexternal mixtures are quite similar to those of the corresponding external mixture. Consequently, semiexternal mixtures may be treated effectively as external mixtures in radiative transfer calculations.

¹Earth Institute at Columbia University, New York, New York, USA.

²NASA Goddard Institute for Space Studies, New York, New York, USA.

³Department of Earth Atmosphere and Planetary Sciences, Massachusetts Institute of Technology, Cambridge, Massachusetts, USA.

⁴Department of Applied Physics and Applied Mathematics, Columbia University, New York, New York, USA.

⁵Max Planck Institute for Chemistry, Mainz, Germany.

Table 1. Refractive Indices at 75% Relative Humidity and 0.7 μm Effective Radius^a

Wavelengths, nm	Dust		Sulfate		Nitrate	
	Real	Imaginary	Real	Imaginary	Real	Imaginary
300	1.600	0.87E-02	1.4247	0.47E-07	1.4205	0.15E-07
550	1.588	0.14E-02	1.4076	0.38E-07	1.4046	0.16E-08
700	1.544	0.07E-02	1.4036	0.60E-07	1.4018	0.25E-07
1000	1.530	0.20E-02	1.3970	0.21E-05	1.3978	0.25E-05
1500	1.510	0.50E-02	1.3850	0.17E-03	1.3893	0.18E-03
2000	1.500	0.80E-02	1.3685	0.11E-02	1.3745	0.10E-02

^aRead 0.87E-02 as 0.87×10^{-2} .

[6] This paper focusses on the optical properties of internal core-mantle mixtures of solid and liquid aerosols. The basic radiative properties of such core-mantle particles are analyzed in section 2. Section 3 describes a global climate model application to study the potential effect of internal mixtures of ammonium sulfate/nitrate and mineral dust particles under present and preindustrial conditions. The main results of the paper are summarized and discussed in section 4.

2. Radiative Properties

[7] A Mie-type code for core-mantle spherical particles [Mishchenko, 1990] was used to calculate the parameters that enter global climate models as the basic radiative characteristics of aerosols: the extinction efficiency, the single-scattering albedo (SSA), and the asymmetry parameter (AP) [Mishchenko et al., 2002]. The size of a composite particle was defined in terms of its outer radius, r . The code was applied to gamma r distributions of two-layer spheres with a fixed ratio ϵ of the shell thickness to the outer radius. Calculations were performed for spherical mineral dust particles covered by a uniform spherical shell of either sulfate, nitrate or water material. The effective radius of the size distribution [see Mishchenko et al., 2002, p. 161] ranged from 0.01 μm to 10 μm and the ratio ϵ ranged from 10% to 100%. The effective variance of the size distribution was fixed at log 2, the wavelength was fixed at 500 nm, and the relative humidity was fixed at 75%. The refractive indices are listed in Table 1 and are taken from the Global Aerosol Climatology Project database (http://gacp.giss.nasa.gov/data_sets) and Mishchenko et al. [1997].

[8] Figure 1 shows the SSA for pure ammonium sulfate and mineral dust aerosols as well as for their internal mixtures. Pure ammonium sulfate particles are nonabsorbing and therefore have SSAs close to unity for all size classes. SSAs of pure mineral dust depend strongly on the particle size and decrease from almost unity for 0.01 μm particles to 0.86 for 10 μm particles. The SSAs of composite particles for all ϵ values tested lie in between the two curves for the pure aerosol types. Therefore sulfate-coated dust particles have SSAs that are lower than those of the pure sulfate aerosols but higher than those of the pure dust particles. The model results further show that if $\epsilon \leq 10\%$ then the corresponding SSAs hardly differ from those of the pure dust aerosols.

[9] The coating layer on the core particle leads to an overall increase in the core-mantle particle size. This effect will partly offset the impact of the increased core-mantle SSA, because SSA decreases with particle size.

[10] The AP results for dust aerosols coated with ammonium sulfate are shown in Figure 1 (bottom). APs of pure ammonium sulfate particles are greater than those of pure dust aerosols. The coated particles have APs lying between those of the pure particles for sizes up to 0.4 μm . However, for larger particles the APs of coated particles are smaller than those for either pure particle type. A smaller AP indicates a more isotropic angular distribution of the scattered light. This occurs, undoubtedly, due to an additional internal optical interface separating the core and the shell which causes additional internal reflections and refractions and serves to randomize the directions of the exiting rays. The smallest AP is found for particles with $\epsilon = 50\%$. If ϵ is smaller than 20%, the resulting APs differ very little from those of pure mineral dust irrespective of particle size. The effect of increased total particle size, due to the coating layer, offsets the discussed effect on AP for particles larger than 0.55 μm , but the increased size effect changes AP more significantly for particles smaller than 0.55 μm .

[11] The extinction efficiency is even less sensitive to coating changes than the displayed parameters in Figure 1 and therefore is not shown. The extinction efficiency is a strong function of particles size. Pure mineral dust shows its largest extinction efficiency at about 0.4 μm particle radii, whereas pure sulfate particles shows its largest extinction efficiency, which is lower than for pure dust, at about 0.5 μm . The coated particles lay in between those two maxima and again the increased size effect will offset the coating effect for particles larger than 0.4 μm .

[12] The results for the ammonium-nitrate-coated dust and water covered dust look very similar and are presented in Figure 1 for the nitrate covered dust.

[13] The above discussed results have been calculated at 550 nm. To test the validity of our results at other wavelengths, aerosol optical properties are calculated at solar wavelengths ranging from 0.2 to 2 μm . This time the particle effective radius was fixed at 0.7 μm and relative humidity at 75%. We display the results for the outer core particle radius of 0.7 μm because coating layers are most relevant for the smallest dust particles (as represented in our climate model), as we will explain later in that paper in section 3. However, larger optical effects may appear at dust sizes smaller than 0.7 μm , which are not included in this study because they are not explicitly represented in our climate model.

[14] Figure 2 shows the results for mineral dust, ammonium sulfate, and sulfate-coated dust particles with a shell thickness ratio of $\epsilon = 10\%$. SSA, AP, and the extinction efficiency are wavelength dependent, but the optical param-

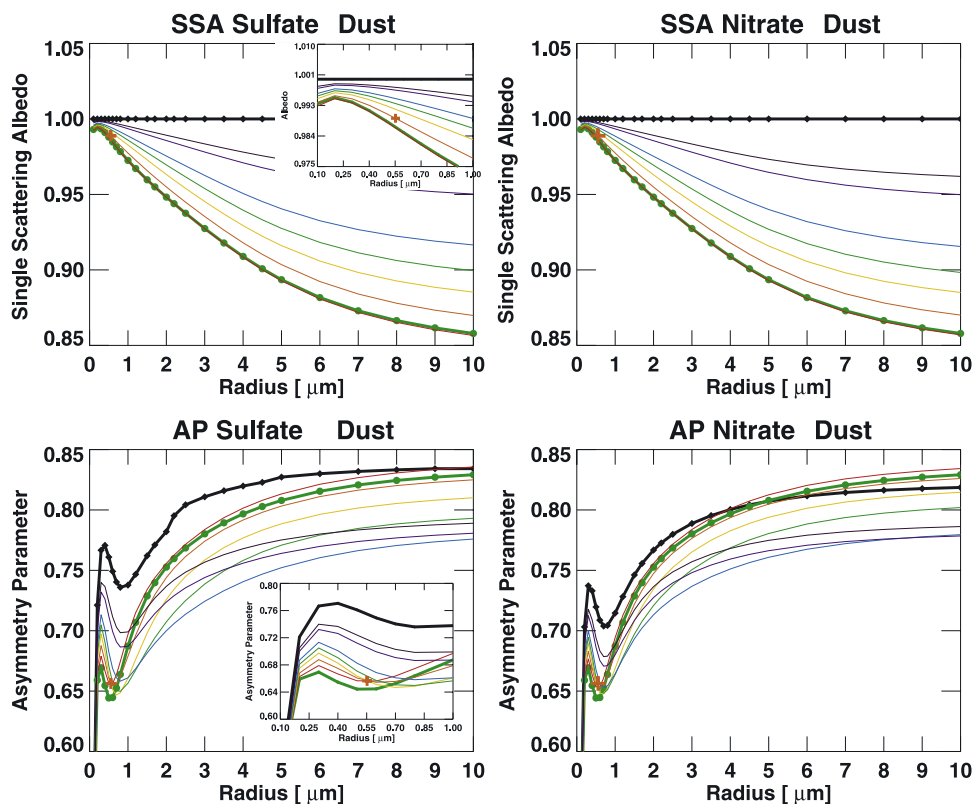


Figure 1. (top) Single-scattering albedo and (bottom) asymmetry parameter for (left) ammonium sulfate dust particles and (right) ammonium nitrate dust particles, as function of particle effective radius [μm], at a fixed wavelength of 550 [nm] and at 75% relative humidity. Results for pure ammonium sulfate, e.g., nitrate (black line with diamonds), pure dust (green line with circles), and dust with 10, 20, 30, 40, 50, 80, and 100% coating of ammonium sulfate/nitrate (red, orange, yellow, green, blue, dark blue, and purple, respectively) are presented.

eters of the coated dust particles differ only slightly from the pure dust particles. Therefore we allow us to study the radiative characteristics of aerosols just for one wavelength, at 550 nm, to be representative for the solar spectrum.

[15] It should be noted that, in reality, dust particles are predominantly nonspherical and are not necessarily located in the center of the composite core-mantle aerosol particles. However, we are looking only at integral scattering and

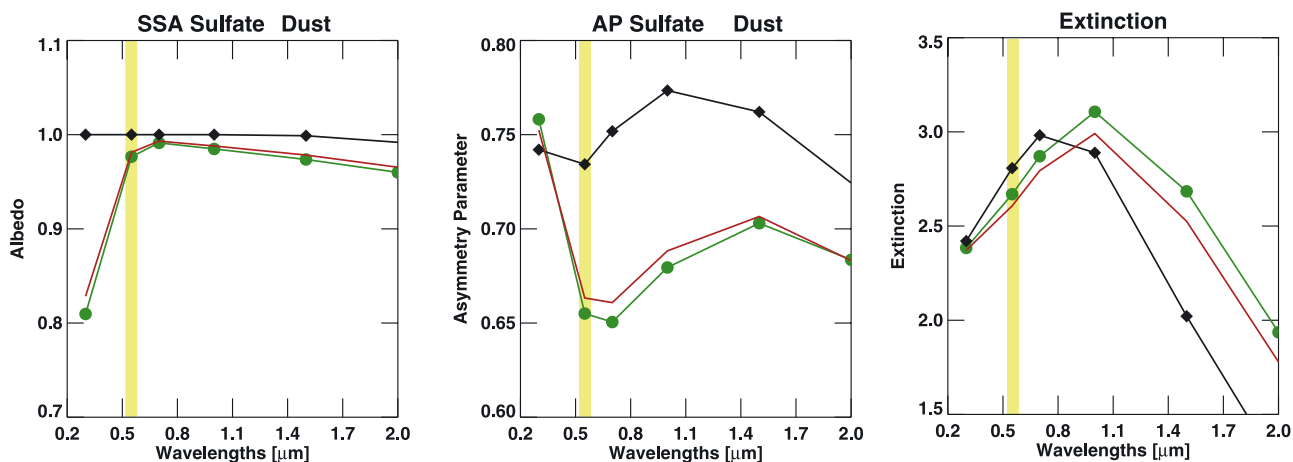


Figure 2. Single-scattering albedo, asymmetry parameter, and extinction efficiency for ammonium sulfate dust particles as a function of wavelengths [μm]. Results for pure ammonium sulfate (black line with diamonds), pure dust (green line with circles), and dust with 10% coating (red line) are presented.

Table 2. Global Annual Budgets

	Present-Day		Preindustrial	
	EXP	CTR	EXP	CTR
Nitrate, Tg N	0.11	0.09	0.05	0.05
Nitrate on dust, Tg N	0.46	-	0.28	-
HNO ₃ , Tg N	3.9	4.2	2.5	2.7
Sulfate, Tg S	0.33	0.48	0.21	0.27
Sulfate on dust, Tg S	0.21	-	0.1	-
Dust, Tg	33.5	41.6	41.8	44.8

absorption characteristics, which should by itself reduce the errors of the assumption that the dust inclusion is located in the center of the composite particle. The papers by *Chylek et al.* [1995] and *Fuller et al.* [1999] indicate that the associated error in the absorption cross section should not exceed 15%. The errors in the other integral optical characteristics can be expected to be even smaller since these quantities are less influenced by the focussing effect that enhances absorption. In addition, the comprehensive analysis by *Mishchenko et al.* [1997] shows that the effects of non-sphericity on the integral optical characteristics should be expected to be of the order of 10% or less.

3. Global Model Study

3.1. Model Description

[16] The Goddard Institute for Space Studies (GISS) general circulation model (GCM) climate model [*Schmidt et al.*, 2006; *Hansen et al.*, 2005] is used in this study to simulate coated mineral dust particles and their implication on climate. The model is employed on a horizontal resolution of $4^\circ \times 5^\circ$ latitude by longitude and 23 vertical layers. The model uses a 30 minute time step for all physics calculations. A complete model description is given by *Schmidt et al.* [2006].

[17] The GCM includes gas phase [*Shindell et al.*, 2003] and aerosol chemistry and carries externally mixed aerosol mass, including sulfate [*Koch et al.*, 2006], nitrate [*Metzger et al.*, 2002b, 2002a], and dust [*Miller et al.*, 2006; *Cakmur et al.*, 2004, 2006], and internally mixed sulfate dust [*Bauer and Koch*, 2005] and nitrate dust particles [*Bauer et al.*, 2004]. Nitrate and sulfate aerosols are transported as mass concentrations and mineral dust aerosols are represented by four size classes: 0.1–1 (clay), 1–2 (silt1), 2–4 (silt2), 4–8 (silt3) μm . Mineral dust emissions are calculated interactively depending on the modeled wind speed and surface conditions. A complete description of mineral aerosols in the GISS GCM is given by *Miller et al.* [2006].

[18] Nitrate and sulfate coatings are allowed to form at all dust particles. Sulfate coated dust particles form through the uptake and oxidation of SO₂ on dust surfaces [*Dentener et al.*, 1996] and this process and model results are described in detail by *Bauer and Koch* [2005] using the GISS GCM. Nitrate aerosol formation is calculated by the thermodynamic equilibrium model EQSAM [*Metzger et al.*, 2002a, 2002b] which is newly implemented into the GISS GCM. The climate model, and respectively the gas phase and other aerosol modules, are linked to EQSAM, by providing sulfate, nitric acid, ammonia, sea salt and gaseous nitrate concentrations as input information for the equilibrium model. The calculated ammonium nitrate aerosols are then

transported, interact with the radiation scheme and are removed by wet and dry deposition within the GCM. Annual mean ammonia concentrations are taken from the EDGAR [*Bouwman et al.*, 1997] emission inventory, on which an artificial annual cycle is superposed on the natural part of the ammonia emissions, to match the seasonal cycle of ammonia, ammonium, and ammonium nitrate measurements. The nitrate formation on dust is calculated as described by *Bauer et al.* [2004], where nitric acid, N₂O₅ and NO₃ can react on mineral dust surfaces and form a stable nitrate coating.

[19] Aerosol optical properties and their coupling to the radiation in the GISS GCM are described by *Koch et al.* [2006], those for externally mixed sulfate aerosols are described by *Koch et al.* [1999], and those for mineral dust are described by *Miller et al.* [2006]. The radiation scheme has the capability to treat size dependence and relative humidity effects on radiative parameters; however, it assumes the aerosols are externally mixed.

[20] The model is run for current climate (with year 2000 emissions, including anthropogenic sources) and preindustrial (year 1750, with natural emission only) climate conditions. Four experiments are carried out: A control experiment (called CTR hereafter) excluding gas-dust interactions and experiment EXP where dust coating is included. Both experiments were run for current climate and preindustrial conditions. The following processes are included in the EXP experiments: (1) Nitrate and sulfate mass are carried as external mixtures and as coatings for each individual dust size bin. (2) The solubility of mineral dust depends on the nitrate and sulfate coating. A dust particle with 10% of its surface area coated is assumed to be completely soluble. This value is taken from *Wyslouzil et al.* [1994] and *Lammel and Novakov* [1995]. In the CTR experiment mineral dust aerosols are treated as insoluble particles. The model was integrated for each experiment for six years and results are shown as average over the last five years.

3.2. Sulfate and Nitrate Coatings

[21] Sulfate and mineral dust interaction are discussed in detail by *Bauer and Koch* [2005]. The paper discusses heterogeneous chemical reactions between sulfate precursors on the surface of mineral dust aerosols affect the atmospheric aerosol cycle and the Earth radiation budget. The global sulfate cycle is influenced by this heterogeneous sulfate formation, which reduces SO₂ concentrations (by about 30% globally), increases total sulfate mass (by about 5%), and reduces externally mixed sulfate aerosols (by about 25%). The anthropogenic sulfate forcing is estimated to be reduced to -0.16 W/m^2 due to the reduced load of externally mixed sulfate aerosols, compared to -0.25 W/m^2 when heterogeneous surface reactions are excluded.

[22] In contrast to the strong impact of heterogeneous sulfate production on the formation of externally mixed sulfate, the total mass of externally mixed nitrate aerosols even increases from 0.09 TgN (CTR) to 0.11 TgN in EXP (see Table 2). Before looking into this phenomena annual mean surface concentrations of total nitrate over North America and Europe are compared (see Figure 3) to observations from the IMPROVE and EMEP network, respectively. Total nitrate is the sum of externally mixed

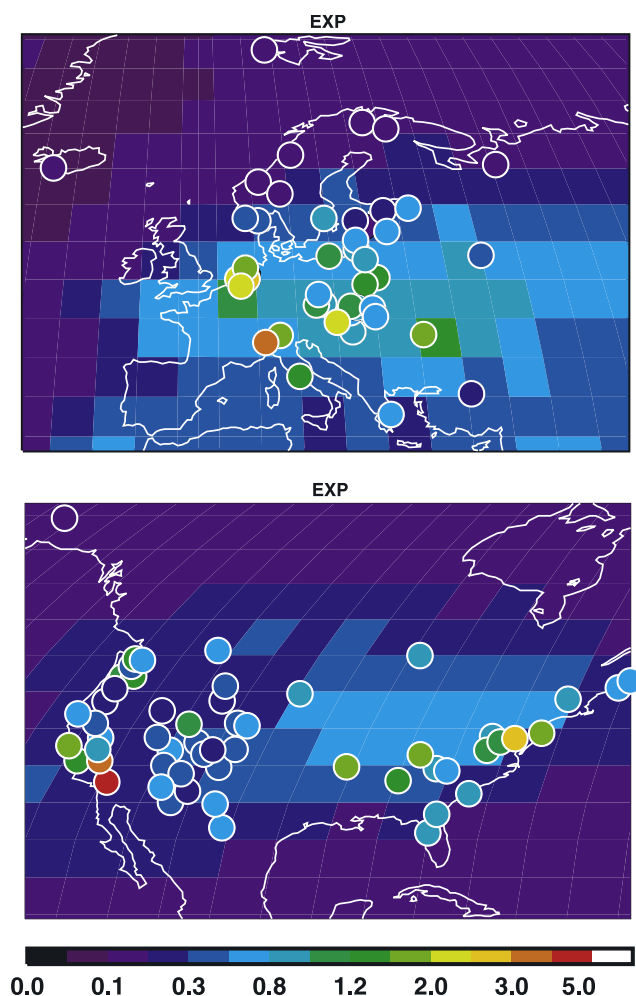


Figure 3. Annual mean surface concentrations of ammonium nitrate. The color-coded circles show measurements as observed by the North American IMPROVE and the European EMEP network. Units are in ppbv.

nitrates and nitrate coatings. The near surface nitrate concentrations agree well over Europe, only some high peak observations cannot be reproduced by the model. The observed concentrations already show large gradients over small distances, these features can as a matter of fact not be reproduced on the coarse horizontal resolution of the model grid. Ammonium nitrate concentrations over North America are slightly underpredicted.

[23] The externally mixed nitrate aerosol mass and the difference between the CTR and the EXP simulation are shown in Figure 4. Most ammonium nitrate is located in the Northern Hemisphere, with maximum concentrations in Asia, Europe and North America. The difference plot shows that nitrate mass increases, in EXP compared CTR, in the Northern Hemisphere, but decreases over India. The main reason for the decrease over India is the strong decrease in nitric acid concentrations in EXP. Nitric acid is an important precursor gas for nitrate formation but as well reacts with the mineral dust surfaces. Globally it is reduced by 8.5% between CTR and EXP, but locally in the Northern African and Arabic regions the reduction is much higher (up to 60% over India). Therefore the reduced amounts of nitric acid in

the EXP simulation lead to a reduced ammonium nitrate aerosol formation. On the other hand externally mixed ammonium nitrate mass is even enhanced in the EXP simulation, especially in the Northern Hemisphere background atmosphere. This is caused by reduced externally mixed sulfate concentrations in EXP. Sulfate can be neutralized by ammonia, the residual amount of ammonia might neutralize nitric acid to form ammonium nitrate. In our EXP simulation the lower sulfate concentration leads to more free ammonia and therefore an enhanced nitrate production. The temperature and humidity conditions are identical in both runs, CTR and EXP.

[24] Figure 5 shows the nitrate that is attached to mineral dust aerosols. The total mass of nitrate coating mineral dust is larger than the amount of externally mixed nitrate (see Table 2). However, the heterogeneous nitrate formation depends strongly on uptake coefficients and the surface areas of the mineral aerosols, both quantities are not well known. Uncertainties regarding heterogeneous sulfate and nitrate formation are discussed and tested in detail by *Bauer et al.* [2004] and *Bauer and Koch* [2005]. The largest amounts of nitrate material coating mineral dust particles are found over northern Africa, Arabia and northern India, but concentrations exceeding 4 mg/m^2 can be found in the Middle Latitudes all over the Northern Hemisphere.

[25] Therefore the contribution of internally mixed nitrates, or in this case nitrates sticking to dust aerosols, is substantial, and the comparisons to the surface observations showed that observed concentrations, in Europe and North America, are still not overestimated by the model. However, it would be very interesting to compare our model results to ammonium nitrate and dust coating measurements in Africa, Arabia and India, to be able to verify the strong nitrate formation we simulate on mineral dust surfaces.

3.3. Impact on Earth Radiation

[26] We are interested in the thickness of the coating layer on the dust particles to determine their optical properties. Figure 6 shows the percentage ratio of sulfate and nitrate thickness material in relation to dust core radius for preindustrial and current climate conditions. We assume that the coating material gets distributed homogeneously over the core particle. The smallest dust particles, clay, experience the largest amount of coating materials on their surface. This is not surprising, as small particles provide the largest surface area and travel over long distances. The thickness of the combined nitrate and sulfate coatings accumulated at all silt particles (all particles larger than $1 \mu\text{m}$) is shown in Figure 6 (right). Dust surface coatings are very small at these larger particles. At present-day conditions coating thickness is lower than 8%, compared to the core particle radius, and lower than 4% at preindustrial times. Coating on clay particles is shown for nitrate coatings only (Figure 6, left) and sulfate coatings (Figure 6, middle). The largest thickness of nitrate coating in relation to dust is found in the Arctic and in the Tropics. The lowest coating thicknesses appear in the regions that have high dust loads, like the Sahara, the Middle East and Australia. Sulfate coating thickness is largest in the Arctic, and quite low everywhere else. Sulfate coatings preliminary develop on East Asian dust and on dust particles that have been transported away from their source region, because sulfate precursors are

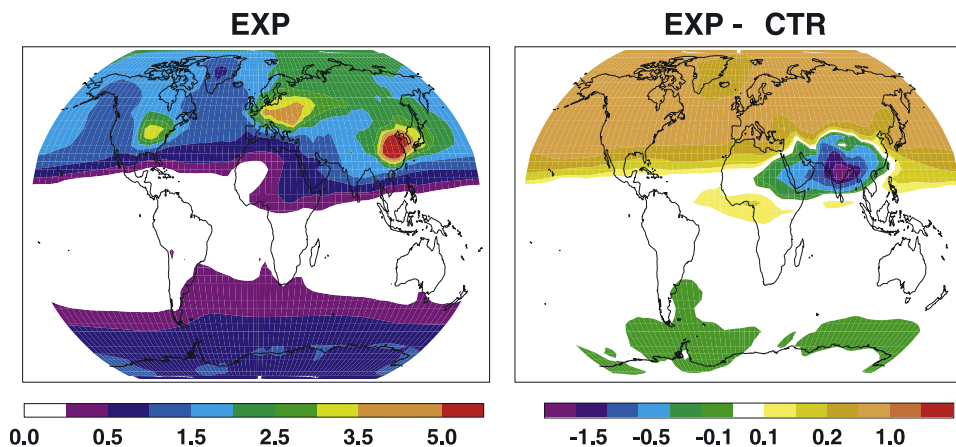


Figure 4. (left) Annual mean column load of externally mixed ammonium nitrate aerosol. (right) Difference between the EXP and the CTR experiment. Units are in mg/m^2 .

mainly released in industrialized regions. Nitrate coatings depend on nitric acid that is formed in polluted regions, but biomass burning and lightning emissions contribute as well substantially to the formation of nitrate coating precursors, therefore there is more nitrate than sulfate material sticking to dust in tropical regions.

[27] However, examining the total thickness of coating material on dust aerosols, we find 20% coating thickness is only exceeded in the Arctic on clay particles, where dust concentrations are extremely low. Coating thickness higher than 10% are found in a wider region, but still in areas with very low dust concentrations. At preindustrial conditions, coating thicknesses are approximately half the size than at present day.

[28] Coatings on dust surfaces lead to an increase in size of the mixed core-mantle particle in relation to the pure dust particle. We argue that this effect is as well negligible on the global scale because significant large coating layers only develop in remote areas with very low dust concentrations, where dust radiative forcing is extremely low anyway, therefore a small change of the optical parameters of the coated dust particles, due to an increased diameter of the core-mantle particle doesn't matter on the global scale.

[29] In summary, only clay particles, in our model particles with radii between 0.1 and 1 μm , experience significant coating which still are smaller than 20% of the core particles radius. We have marked these particles with an orange cross in Figure 1. Considering the fact that coating thicknesses are much smaller (between 0 and 5%) in dust regions, we conclude that optical properties of coated dust particles do not differ substantially from uncoated particles. Therefore all mineral dust particles can be treated as pure in the radiation scheme.

4. Results and Discussion

[30] This paper discusses the radiative properties of sulfate and nitrate coated, humid mineral dust particles. The overall result of this study is, that significant coating layers, that could effect the radiative properties of dust particles only occur in regions with very low dust loads.

Therefore the direct radiative effect of coatings on dust aerosols may be neglected in global climate models.

[31] To validate the discussed model simulations, detailed observations are necessary, describing the shape and chemical composition of single particles. *Mamane and Noll* [1985] and *Mamane et al.* [1992] analyzed particles collected in North Carolina, United States, with electron microscopy and they found sulfate coatings on calcite and clay minerals on the order of 1–2.7% in relation to the core particle. In a laboratory experiment [*Mamane and Gottlieb*, 1992], nitrate-coated dust particles were observed. The concentration of minerals was around 1–3 $\mu\text{g m}^{-3}$ and no more than 0.01–0.24 $\mu\text{g m}^{-3}$ of nitrate was found on the dust particles surfaces.

[32] The result of this study is, that coatings on mineral dust particles do not change significantly the radiative properties of dust aerosols. Nevertheless, we want to point out, that heterogeneous surface reactions play a very important role in direct radiative forcing, because the loads of the individual aerosol species are changed by these reactions. For example, the deliquescence of the mixed dust is increased by soluble coatings sticking to an insoluble dust

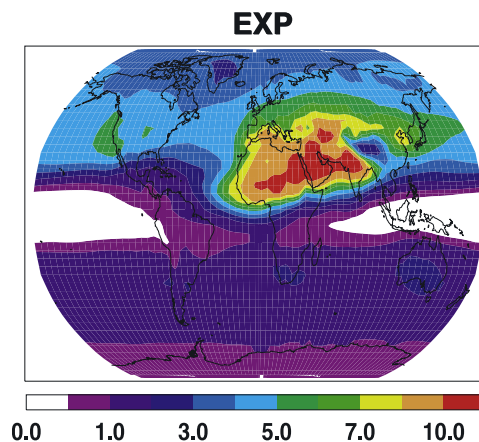


Figure 5. Annual mean column load of ammonium nitrate attached to mineral dust. Units are in mg/m^2 .

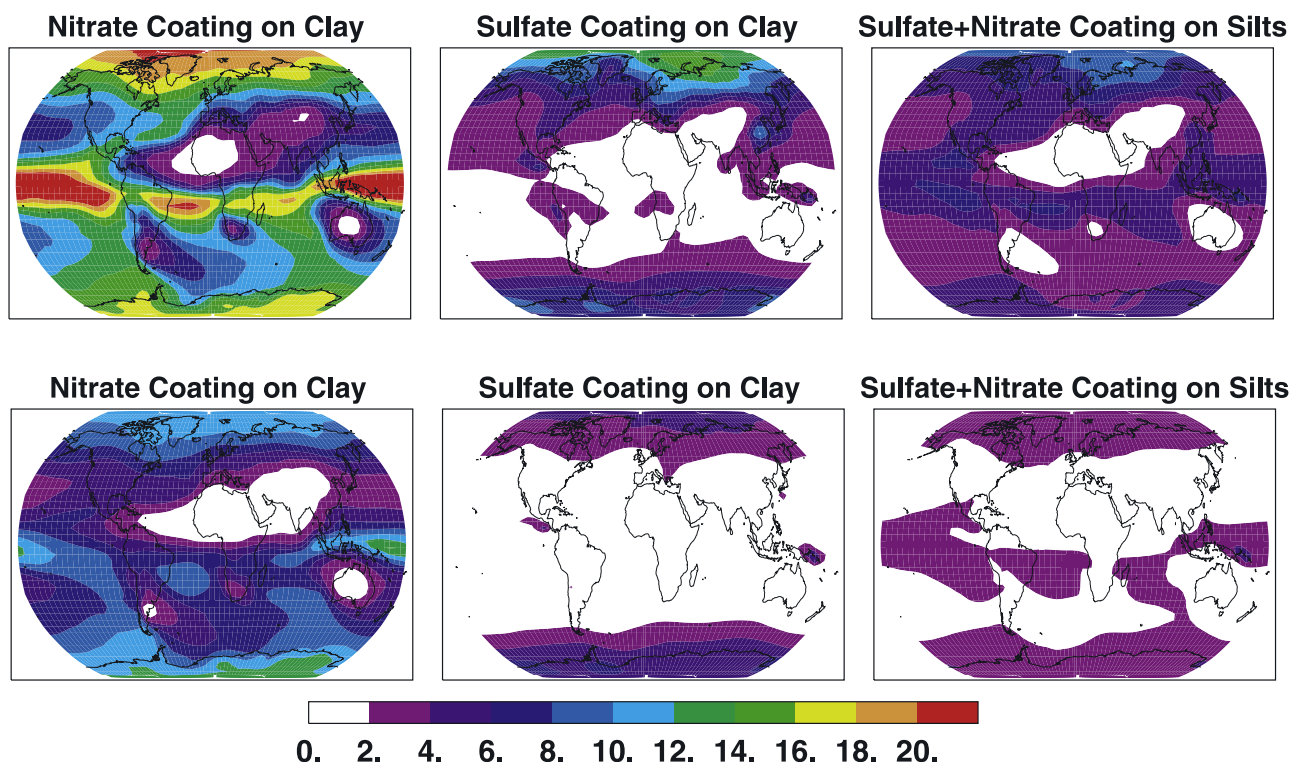


Figure 6. Annual mean ratio of shell material thickness in relation to dust core radius. Units are in percentage. Results are shown for (top) current climate and (bottom) preindustrial climate conditions. The ratio for (left) nitrate coating and (middle) sulfate coating is shown for clay particles and (right) the combined nitrate and sulfate coating for silt particles.

core. This process leads to a shorter lifetime of dust under current climate conditions compared to preindustrial times.

[33] Table 3 gives the contribution of the global top of the atmosphere radiative forcing for the three different aerosol types discussed in this study. Radiative forcings are given for present-day conditions, and anthropogenic change including and excluding heterogeneous surface reactions. In our experiments we used the same dust emission sources for both episodes, therefore the changes in the dust load are caused by the differences in dust solubility. The anthropogenic impact reduced the dust aerosol attributed top of the atmosphere cooling by 0.23 W/m^2 compared to preindustrial times, due to the reduced load of reflective mineral dust material at present times. The longwave forcing is changed by -0.11 W/m^2 . That leads to a total change of 0.12 W/m^2 in dust radiative forcing.

[34] Our sulfate aerosol radiative forcing is smaller at present-day conditions than in most other studies [Kinne *et al.*, 2006]. This is caused mainly by the cloud tracer budget [Koch *et al.*, 2003] and secondarily by the reduced production of externally mixed aerosols [Bauer and Koch, 2005]. Sulfate precursors are as well consumed by heterogeneous reactions, which lowers the productions of externally mixed sulfate aerosols. The anthropogenic forcing of sulfates are reduced from -0.25 to -0.16 W/m^2 due to the impact of the dust coating process.

[35] The formation of externally mixed nitrate aerosols is not changed as significantly by coating processes. The anthro-

pogenic forcing of nitrates only varies by -0.01 W/m^2 between the CTR and EXP experiment.

[36] Although, the magnitude is uncertain, we want to point out that the radiative cooling effects of the reflective aerosols are strongly reduced. Adding up the numbers in Table 3, the combined radiative forcing is -0.1 W/m^2 . Neglecting surface coating processes, the combined nitrate and sulfate forcing adds up to -0.3 W/m^2 .

[37] Figure 7 compares the total aerosol optical thickness (AOT) of the two model runs CTR and EXP to the annual mean aerosol optical thickness as observed by the AERONET Sun photometer network of the year 2000. EXP shows lower AOT, especially over the Sahara, Europe and North America. All these reductions in AOT agree better with the observations. The reduced AOT over northern Africa is caused by the increased solubility of mineral dust in EXP, explaining its reduced lifetime. We are aware of the strong temporal fluctuations in mineral dust loads, and

Table 3. Top of the Atmosphere Radiative Forcing^a

	Present-Day 2000	Anthropogenic Change 2000–1750	Anthropogenic Change Without Coating 2000–1750
Sulfate	-0.43	-0.16	-0.25
Nitrate	-0.11	-0.06	-0.05
Dust (short wave)	-0.76	0.23	-
Dust (long wave)	0.25	-0.11	-

^aValues are in W/m^2 .

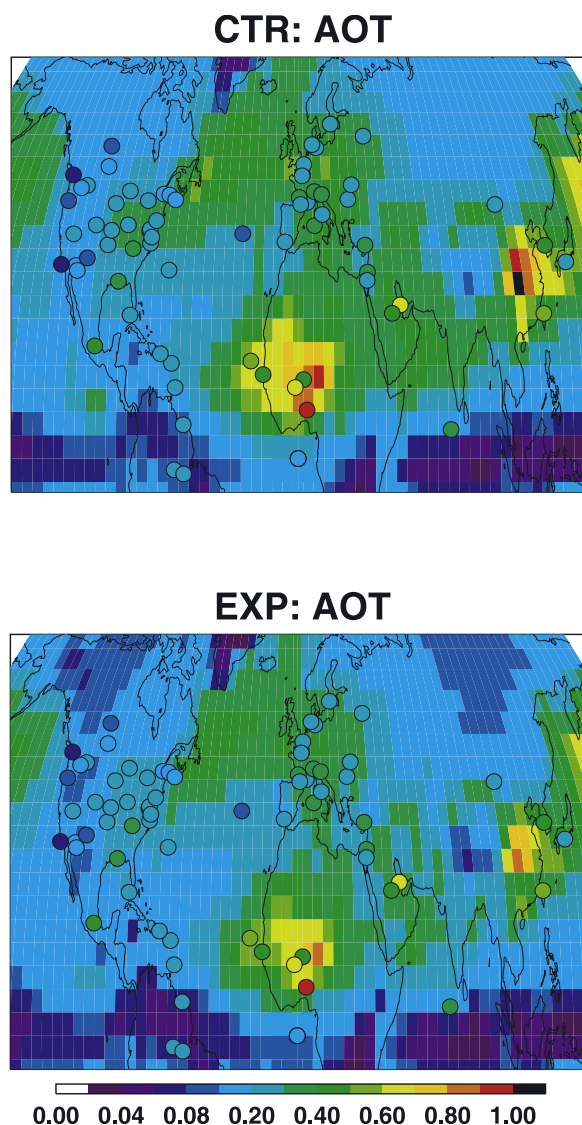


Figure 7. Annual mean aerosol optical thickness for the (top) CTR and (bottom) EXP. The color-coded circles show optical thickness as measured by AERONET.

therefore comparisons over the Sahara must be done very carefully. However, the reduced loads of nitrate and sulfate pollutants over the Industrial regions may be more meaningful. Nevertheless, only detailed chemical analysis of single aerosol particles can determine if our simulations show the correct estimates of this effect.

[38] In summary, anthropogenic climate warming is much less counter balanced by scattering aerosols than previously expected when dust coating effects are included in the calculations. For future projections we assume that heterogeneous reactions affecting aerosols become even more important, due to the predicted increase of SO_2 emissions in the developing world, and the global increase in nitrogen and ammonia emissions.

[39] This study only focused on the direct aerosol impact, but likewise significant effects can be expected for aerosol-cloud interactions.

[40] **Acknowledgments.** We like to thank Nadine Unger for providing the emission data sets for the present-day and preindustrial simulations. We thank Sarah Guilbert and Stefan Kinne for their help with the AERONET data set. We acknowledge AERONET, IMPROVE, and EMEP network. This work has been supported by the NASA MAP program Modeling, Analysis, and Prediction Climate Variability and Change (NN-H-04-2-YS-008-N).

References

- Bauer, S. E., and D. Koch (2005), Impact of heterogeneous sulfate formation at mineral dust surfaces on aerosol loads and radiative forcing in the GISS GCM, *J. Geophys. Res.*, *110*, D17202, doi:10.1029/2005JD005870.
- Bauer, S. E., Y. Balkanski, M. Schulz, D. A. Hauglustaine, and F. Dentener (2004), Global modelling of heterogeneous chemistry on mineral aerosol surfaces: The influence on tropospheric ozone chemistry and comparison to observations, *J. Geophys. Res.*, *109*, D02304, doi:10.1029/2003JD003868.
- Bouwman, A. F., D. S. Lee, W. A. H. Asman, F. J. Dentener, K. W. V. D. Hoek, and J. Olivier (1997), A global high-resolution emission inventory for ammonia, *Global Biogeochem. Cycles*, *11*, 561–587.
- Buseck, P. R., and M. Posfai (1999), Airborne minerals and related aerosol particles: Effects on climate and the environment, *Proc. Natl. Acad. Sci. U. S. A.*, *96*, 3372–3379.
- Buseck, P. R., D. J. Jacob, M. Posfai, J. Li, and J. Anderson (2000), Minerals in the air: An environmental perspective, *Int. Geol. Rev.*, *42*, 577–593.
- Cakmur, R., R. L. Miller, and O. Torres (2004), Incorporating the effect of small-scale circulations upon dust emission in an atmospheric general circulation model, *J. Geophys. Res.*, *109*, D07201, doi:10.1029/2003JD004067.
- Cakmur, R. V., R. L. Miller, J. Perlwitz, I. V. Geogdzhayev, P. Ginoux, D. Koch, I. Tegen, and C. S. Zender (2006), Constraining the magnitude of the global dust cycle by minimizing the difference between a model and observations, *J. Geophys. Res.*, *111*, D06207, doi:10.1029/2005JD005791.
- Chýlek, P., G. Videen, D. Ngo, R. G. Pinnick, and J. D. Klett (1995), Effect of black carbon on the optical properties and climate forcing of sulfate aerosols, *J. Geophys. Res.*, *100*, 16,325–16,332.
- Dentener, F. J., G. R. Carmichael, Y. Zang, J. Lelieveld, and P. J. Crutzen (1996), Role of mineral aerosol as a reactive surface in the global troposphere, *J. Geophys. Res.*, *101*, 22,869–22,889.
- Fuller, K. A., W. Malm, and S. Kreidenweis (1999), Effects of mixing on extinction by carbonaceous particles, *J. Geophys. Res.*, *104*, 15,941–15,954.
- Gong, S. L., et al. (2003), Canadian aerosol module: A size-segregated simulation of atmospheric aerosol processes for climate and air quality models: 1. Module development, *J. Geophys. Res.*, *108*(D1), 4007, doi:10.1029/2001JD002002.
- Hansen, J., et al. (2005), Efficacy of climate forcing, *J. Geophys. Res.*, *110*, D18104, doi:10.1029/2005JD005776.
- Jacobson, M. Z. (2001), Global direct radiative forcing due to multicomponent anthropogenic and natural aerosols, *J. Geophys. Res.*, *106*, 1551–1568.
- Kinne, S., et al. (2006), An AeroCom initial assessment optical properties in aerosol component modules of global models, *Atmos. Chem. Phys.*, *6*, 1815–1834.
- Koch, D., D. Jacob, I. Tegen, D. Rind, and M. Chin (1999), Tropospheric sulfur simulation and sulfate direct radiative forcing in the Goddard Institute for Space Studies general circulation model, *J. Geophys. Res.*, *104*, 23,799–23,822.
- Koch, D., J. Park, and A. D. Genio (2003), Clouds and sulfate are anticorrelated: A new diagnostic for global sulfur models, *J. Geophys. Res.*, *108*(D24), 4781, doi:10.1029/2003JD003621.
- Koch, D., G. Schmidt, and C. Field (2006), Sulfur, sea salt, and radionuclide aerosols in the GISS ModelE, *J. Geophys. Res.*, *111*, D06206, doi:10.1029/2004JD005550.
- Lammel, G., and T. Novakov (1995), Water nucleation properties of carbon black and diesel soot particles, *Atmos. Environ.*, *29*, 813–823.
- Li, J., J. R. Anderson, and P. R. Buseck (2003a), TEM study of aerosol particles from clean and polluted marine boundary layers over the North Atlantic, *J. Geophys. Res.*, *108*(D6), 4189, doi:10.1029/2002JD002106.
- Li, J., M. Posfai, P. Hobbs, and P. R. Buseck (2003b), Individual aerosol particles from biomass burning in southern Africa: 2 Compositions and aging of inorganic particles, *J. Geophys. Res.*, *108*(D13), 8484, doi:10.1029/2002JD002310.
- Mamane, Y., and J. Gottlieb (1992), Nitrate formation on sea-salt and mineral particles: A single particle approach, *Atmos. Environ., Part A*, *26*, 1763–1769.

- Mamane, Y., and K. E. Noll (1985), Characterization of large particles at a rural site in the eastern United States: Mass distribution and individual particle analysis, *Atmos. Environ.*, *19*, 611–622.
- Mamane, Y., T. G. Dzubay, and R. Ward (1992), Sulfur enrichment of atmospheric minerals and spores, *Atmos. Environ., Part A*, *26*, 1113–1120.
- Metzger, S. M., F. J. Dentener, A. Jeuken, M. Krol, and J. Lelieveld (2002a), Gas/aerosol partitioning: 2. Global model results, *J. Geophys. Res.*, *107*(D16), 4313, doi:10.1029/2001JD001103.
- Metzger, S. M., F. J. Dentener, J. Lelieveld, and S. N. Pandis (2002b), Gas/aerosol partitioning: 1. A computationally efficient model, *J. Geophys. Res.*, *107*(D16), 4312, doi:10.1029/2001JD001102.
- Miller, R. L., et al. (2006), Mineral dust aerosols in the NASA Goddard Institute for Space Sciences ModelE atmospheric general circulation model, *J. Geophys. Res.*, *111*, D06208, doi:10.1029/2005JD005796.
- Mishchenko, M. (1990), Expansion of scattering matrix in generalized spherical harmonics for radially inhomogeneous spherical particles, *Kinematica Fiz. Nebesnykh Tel*, *6*, 93–95.
- Mishchenko, M., L. D. Travis, R. A. Kahn, and R. A. West (1997), Modeling phase functions for dustlike tropospheric aerosols using a shape mixture of randomly oriented polydisperse spheroids, *J. Geophys. Res.*, *102*, 16,831–16,847.
- Mishchenko, M., L. D. Travis, and A. A. Lacis (2002), *Scattering, Absorption, and Emission of Light by Small Particles*, Cambridge Univ. Press, New York.
- Mishchenko, M., B. Cairns, J. E. Hansen, L. D. Travis, R. Burg, Y. J. Kaufman, J. V. Martins, and E. P. Shettle (2004a), Monitoring of aerosol forcing of climate from space: Analysis of measurement requirements, *J. Quant. Spectrosc. Radiat. Transfer*, *88*, 149–161.
- Mishchenko, M., L. Liu, L. D. Travis, and A. A. Lacis (2004b), Scattering and radiative properties of semi-external versus external mixtures of different aerosol types, *J. Quant. Spectrosc. Radiat. Transfer*, *88*, 139–147.
- Schmidt, G. A., et al. (2006), Present day atmospheric simulations using GISS ModelE: Comparison to in-situ, satellite and reanalysis data, *J. Clim.*, *19*, 153–192.
- Shindell, D. T., G. Faluvegi, and N. Bell (2003), Preindustrial-to-present-day radiative forcing by tropospheric ozone from improved simulations with the GISS chemistry-climate GCM, *Atmos. Chem. Phys.*, *3*, 1675–1702.
- Stier, P., et al. (2005), The aerosol-climate model ECHAM5-HAM, *Atmos. Chem. Phys.*, *5*, 1125–1156.
- Trochine, D., Y. Iwasaka, A. Matsuki, M. Yamada, Y.-S. Kim, T. Nagatani, D. Zhang, G.-Y. Shi, and Z. Shen (2003), Mineral aerosol particles collected in Dunhuang, China, and their comparison with chemically modified particles collected over Japan, *J. Geophys. Res.*, *108*(D23), 8642, doi:10.1029/2002JD003268.
- Wyslouzil, B. E., K. L. Carleton, D. M. Sonnenfroh, W. T. Rawlins, and S. Arnold (1994), Observation of hydration of single, modified carbon aerosols, *Geophys. Res. Lett.*, *21*, 2107–2110.

S. E. Bauer, A. A. Lacis, and M. I. Mishchenko, NASA Goddard Institute for Space Studies, 2880 Broadway, New York, NY 10025, USA. (sbauer@giss.nasa.gov)

S. M. Metzger, Max Planck Institute for Chemistry, P. O. Box 3060, D-55020 Mainz, Germany.

J. Perlwitz, Department of Applied Physics and Applied Mathematics, Columbia University, 500 West 120th Street, New York, NY 10027, USA.

S. Zhang, Department of Earth Atmosphere and Planetary Sciences, Massachusetts Institute of Technology, Cambridge, MA 02139, USA.